AUTOMATIC, EXPLORATORY MINERALOGICAL MAPPING OF CRISM IMAGERY CONTAINING GULLY FEATURES. E. J. Allender[1] and T. F. Stepinski[1], [1]Space Informatics Lab, University of Cincinnati, 2600 Clifton Ave, Cincinnati, 45221. (allendej@mail.uc.edu).

Introduction: Many processing methods exist to extract mineralogical information from Compact Reconnaissance Imaging Spectrometer for Mars (CRISM) images [1, 2, 3], however, such methods are not designed with large-scale, exploratory surveys in mind. Typically, for manual analyses mineral information must be provided a priori (that is, analysts must know in advance the mineral type they are looking for) in order to select an appropriate RGB combination of CRISM summary products [4, 5] for visualization. If spectral unmixing is to be performed as in [3], the number of potential mineral endmembers must be assumed a priori. Regardless of whether manual analysis or unmixing takes place, resulting mineral units and endmembers must be matched to a spectral library for identification, using either visual [6], or distance-based [7] methods.

We present a fully-automated processing pipeline which is able to take a raw CRISM TRR3 image as input, and produce a classified and labeled map of interesting mineralogy within an image.

Extending the survey performed by [8], we intend to perform a global survey of all 450 gully-containing CRISM images, which overlap observations from [9], and examine the mineral content of these images in order to determine if gully formations may be associated with some hydrated mechanism. The existence of any mineralogical association with orientation, region, or latitude will also be investigated.

Automated pipeline: The pipeline requires no user input other than the initial download of TRR3 images and their arrangement into a simple directory structure. Unlike manual and unmixing methods, no a priori knowledge is required to implement the pipeline – in place of a traditional hyperspectral signature, we use the entire suite of band-depth-based summary products [4, 5] to capture key absorption features at each pixel. This way, no tri-color CRISM summary product combinations need to be selected a priori, as is usually performed for mineral visualization, because we utilize all summary products relevant to surface mineralogy at the same time. Additionally, due to the algorithms [10, 11] we have chosen for the mineral detection and exemplar identification stage, we are able to automatically estimate the number of 'interesting' mineral types within an image. Following each run of the pipeline, *exemplar* signatures – each of which represent an 'interesting' mineral type present in an image – may be queried with respect to their mineral type. This greatly facilitates exploratory analysis as hundreds of images need not be manually searched by an analyst looking for a specific mineral type. Instead, they may query a mineral type of interest (for example, Mg-Carbonate), and be presented with a list of FRTs containing evidence for this mineral.

The pipeline operates in stages, as follows:

Stage 1. Pre-processing: The pipeline is initialized in the GRASS GIS environment [12] with a single command and performs all standard pre-processing steps using CRISM ANALYSIS TOOLKIT (CAT) procedures. IR summary products are also generated for each image. At the end of this stage, each image is represented by a raster, in which each pixel contains a vector of 18 (surface-related) summary product responses. Pre-processed images are passed through a control script which calls all subsequent processing stages whose components are written in C, R and bash.

Stage 2. Segmentation: Graph-based segmentation [13] is then performed to segment the image into homogeneous regions called 'superpixels'. The mean signatures of these superpixels are the input for subsequent processing stages.

Stage 3. Mineral detection and exemplar identification: We use the DEMUD algorithm [10] to identify the most unique superpixel signatures within each image, and the OPTICS clustering algorithm [11] to eliminate redundancy within this set and to output a final set of exemplars representing mineralogical units to be mapped.

Stage 4. Mineral type labeling: Using a custom LookUp-Table (LUT) based on summary product sensitivities from [5] a mineral type is assigned to each exemplar based on the elements of its summary product signature that are enhanced with respect to the overall image. A text file containing the labeled exemplars is output along with a map of their spatial distribution for each image.

Stage 5 (optional). Mineralogical query: In order to make use of the output from the labeling stage when processing a large number of sites we have additionally built in a search function, so that a user may query a mineral type of interest and obtain a text file containing the names of all FRTs in which evidence for that mineral type has been detected.

Preliminary results: Initial testing was performed on 20 sites containing a range of surface features (not only gullies) whose content has previously been docu-

mented using manual methods [6, 14, 15, 16, 17]. Figure 1 shows our pipeline output for FRT3E92, an image from the initial testing phase manually studied by [14], who specifically set out to analyze phyllosilicate content at the site. We produced this map with no a priori knowledge of its content, and made no a priori assumptions as to how many mineral types may be present. The image was simply presented to the pipeline, and the map was output along with a labeled file describing the interesting mineral types detected. We were not limited to the detection of any particular type based on the selection of summary products used, as [14] was.

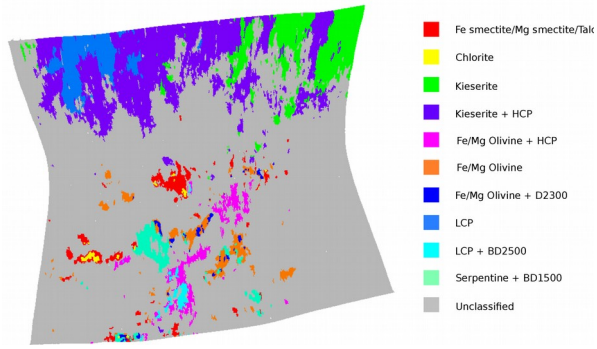

Figure 1: Output map for testing image FRT3E92.

Based on encouraging results from the testing phase we have now progressed to exploring 100 CRISM images containing poleward-facing gully formations. These 100 sites are only a subset of our eventual goal of processing all 450 CRISM images containing gullies of a variety of orientations from [9] to investigate whether a hydrated mechanism may have played a role in their formation, or if any mineralogical association exists with orientation, region, or latitude. The current subset of 100 poleward-facing sites covers the Terra Sirenum, Aonia Terra, Noachis Terra, Argyre Basin, and Hellas Basin regions, from -30 to -50 degrees latitude.

88 of the 100 gully-containing sites were found to contain interesting mineral types, as shown in Figure 2. These sites are labeled to highlight sites displaying evidence of hydrated mineralogy.

From this figure no strong correlation with latitude or region is observed, however, at present we present only the preliminary results of our global survey.

Each of the 88 images containing mineral types of interest were individually examined to determine whether any mineral units were associated with gully features. Of the 51 images containing both hydrated and mafic minerals, only 17 had deposits associated with gully features. Of the 36 images containing only mafic minerals, 25 were associated with gully features. The single image containing only hydrated mineralogy was not associated with any gully features. Therefore, like [8] we suppose that the presence of hydrated mineralogy within gully features is a result of the exposure of underlying mineral deposits and not a result of the gully formation mechanism - gullies generally appear to be spectrally indistinct from their surroundings, as evidenced by the large number associated with mafic mineralogy.

Ultimately, use of our pipeline will greatly facilitate exploratory analysis and large-scale image surveys, as hundreds of images need not be manually searched by an analyst looking for a specific mineral type. We have preliminarily demonstrated this on a subset of 100 gully-containing CRISM images, and plan to continue our exploration at a global scale.

References: [1] Murchie et al. (2007), *JGR: Planets*, *112 E5*. [2] Ehlmann et al. (2009), *JGR*, *114*, E00D08. [3] Mandrake et al. (2010), LPSC 2010, Abstract #1441. [4] Pelkey et al. (2007), *JGR*, *112*, E8, 1-18. [5] Viviano-Beck et al. (2014), *JGR*, *119(6)*, 1403-1431. [6] Bishop et al. (2009), JGR, 114, E00D09. [7] Thomas et al. (2014), LPSC 2014, Abstract #1909. [8] Nunez et al. (2014), Eighth Int. Conf. Mars. Abstract #1486. [9] Harrison et al. (2015), *Icarus*, *252*, 236-254. [10] Wagstaff et al. (2013), Proc. AIII-13, 1-7. [11] Ankerst et al. (1999), Proc. ACM SIGMOD '99. [12] GRASS Dev. Team, GRASS Software V6.4.4, OSGF. [13] Felzenschwalb & Huttenlocher. (2004), I*nt. Journal. Comp. Vision*, *59(2)*, 167-181. [14] Mustard et al. (2008), *Nature*, *454(7202)*, 305-309. [15] Lichtenberg et al. (2010), *JGR*, *115*, E00D17. [16] Noe Dobrea et al. (2010), *JGR*, *115*, E00D19. [17] Ackiss & Wray. (2014), *Icarus*, *243*, 311-324.

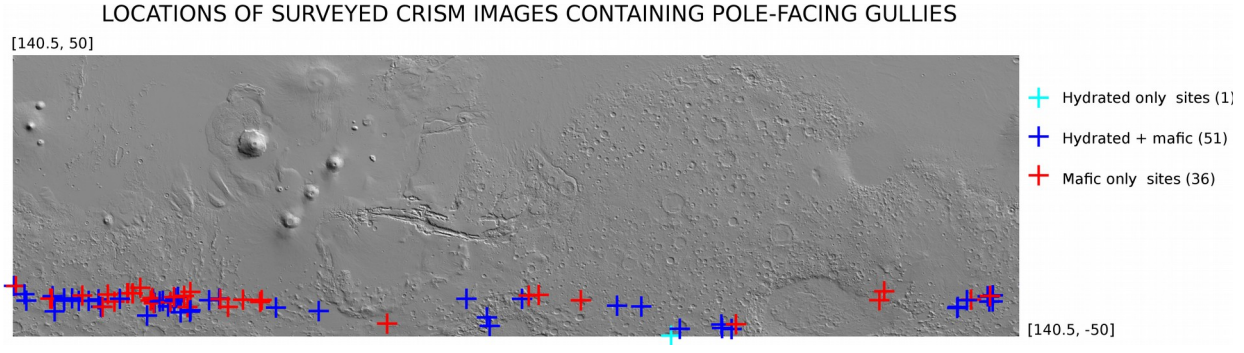

Figure 2: 88 of 100 sites containing 'interesting' mineral types, labeled according to hydrated/mafic content. Note that 88 sites are not visible in this map – this is because some FRTs overlap, and to preserve clarity only a single symbol was used to represent them.